# Cytochrome P450 associated with insecticide resistance catalyzes cuticular hydrocarbon production in *Anopheles gambiae*

Vasileia Balabanidou[a,b], Anastasia Kampouraki[b], Marina MacLean[c], Gary J. Blomquist[c], Claus Tittiger[c], M. Patricia Juárez[d], Sergio J. Mijailovsky[d], George Chalepakis[b], Amalia Anthousi[b], Amy Lynd[e], Sanou Antoine[e], Janet Hemingway[e,1], Hilary Ranson[e], Gareth J. Lycett[e], and John Vontas[a,f,1]

[a]Institute of Molecular Biology and Biotechnology, Foundation for Research and Technology-Hellas, Heraklion 70013, Greece; [b]Department of Biology, University of Crete, Vassilika Vouton, Heraklion 70013, Greece; [c]Department of Biochemistry and Molecular Biology, University of Nevada, Reno, NV 89557; [d]Instituto de Investigaciones Bioquímicas de La Plata, Centro Científico Tecnológico La Plata, Consejo Nacional de Investigaciones Científicas y Técnicas - Facultad de Ciencias Médicas, Universidad Nacional de La Plata, La Plata 1900, Argentina; [e]Department of Vector Biology, Liverpool School of Tropical Medicine, Liverpool L3 5QA, United Kingdom; and [f]Pesticide Science Laboratory, Department of Crop Science, Agricultural University of Athens, 11855 Athens, Greece

Contributed by Janet Hemingway, June 14, 2016 (sent for review February 26, 2016); reviewed by Jeffrey Bloomquist, Basil D. Brooke, and Pie Mueller

**The role of cuticle changes in insecticide resistance in the major malaria vector *Anopheles gambiae* was assessed. The rate of internalization of $^{14}$C deltamethrin was significantly slower in a resistant strain than in a susceptible strain. Topical application of an acetone insecticide formulation to circumvent lipid-based uptake barriers decreased the resistance ratio by ∼50%. Cuticle analysis by electron microscopy and characterization of lipid extracts indicated that resistant mosquitoes had a thicker epicuticular layer and a significant increase in cuticular hydrocarbon (CHC) content (∼29%). However, the CHC profile and relative distribution were similar in resistant and susceptible insects. The cellular localization and in vitro activity of two P450 enzymes, CYP4G16 and CYP4G17, whose genes are frequently overexpressed in resistant *Anopheles* mosquitoes, were analyzed. These enzymes are potential orthologs of the CYP4G1/2 enzymes that catalyze the final step of CHC biosynthesis in *Drosophila* and *Musca domestica*, respectively. Immunostaining indicated that both CYP4G16 and CYP4G17 are highly abundant in oenocytes, the insect cell type thought to secrete hydrocarbons. However, an intriguing difference was indicated; CYP4G17 occurs throughout the cell, as expected for a microsomal P450, but CYP4G16 localizes to the periphery of the cell and lies on the cytoplasmic side of the cell membrane, a unique position for a P450 enzyme. CYP4G16 and CYP4G17 were functionally expressed in insect cells. CYP4G16 produced hydrocarbons from a C18 aldehyde substrate and thus has bona fide decarbonylase activity similar to that of dmCYP4G1/2. The data support the hypothesis that the coevolution of multiple mechanisms, including cuticular barriers, has occurred in highly pyrethroid-resistant *An. gambiae*.**

malaria | insecticide resistance | hydrocarbons | mosquito cuticle | cytochrome P450

Pyrethroid resistance in malaria vectors of human disease is at a critical tipping point. Resistance is now widespread and is rapidly increasing in intensity in *Anopheles* mosquitoes across Africa (1, 2). A key challenge is to maintain the efficacy of current interventions in the face of growing insecticide resistance. Overexpression of detoxification enzymes, which inactivate or sequester insecticides, and mutations in the target site that alter the affinity of insecticide binding have been widely described in the major malaria vector *Anopheles gambiae* (3). However, the emergence of striking multiple-resistant phenotypes in West Africa, where mosquito populations with very high pyrethroid resistance levels are also resistant to additional classes of insecticides (4–6), suggests the emergence of additional broad-spectrum mechanisms.

The cuticle has been hypothesized to play a role in insecticide resistance via modifications that reduce or slow insecticide uptake. The phenomenon has been studied in some agricultural pests (7–9). Cuticle thickening, hydrocarbon (HC) content, and reduced deltamethrin penetration have been associated with high levels of pyrethroid resistance in the hemipteran *Triatoma infestans*, the vector of Chagas disease in the Americas (10, 11), and cuticular resistance has been demonstrated in a dichloro-diphenyl-trichloroethane (DDT)-resistant *Drosophila* strain (12). Cuticular resistance has been hypothesized in mosquitoes, but empirical data are confined to a report that increased cuticle thickness is associated with pyrethroid resistance in *Anopheles funestus* (13). Transcriptomic studies show substantial overexpression of multiple cuticular genes in several resistant *Anopheles* and *Aedes* mosquito populations (14–16). Genes possibly involved in the biosynthesis of lipid components and fatty acid metabolism are also associated with resistant phenotypes in *Anopheles arabiensis* and *An. gambiae* (16, 17). In particular, the cytochrome P450 *cyp4g16* and *cyp4g17* genes are overexpressed in resistant populations of both *An. gambiae* (18) and *An. arabiensis* (17) in several regions in Africa.

Unlike the *Anopheles* P450 cytochromes agCYP6M2 and agCYP6P3, which are localized primarily in Malpighian tubules and the mosquito gut (19, 20) and metabolize pyrethroids, no

## Significance

Malaria incidence has halved since 2000, with 80% of the reduction attributable to the use of insecticides, which now are under threat of resistance. Understanding the mechanisms of insecticide resistance is a key step in delaying and tackling the phenomenon. This study provides evidence of a cuticular mechanism that slows the uptake of pyrethroids, contributing to the resistance phenotype and potentially broadening resistance to multiple insecticide classes, thus providing additional challenges to resistance management. Quantitative modification of cuticular hydrocarbons is associated with increased expression of a 4G cytochrome P450 enzyme, CYP4G16, which catalyzes epicuticular hydrocarbon biosynthesis. This work improves our understanding of insecticide resistance and may facilitate the development of insecticides with greater specificity to mosquitoes and greater potency.

Author contributions: V.B., A.K., M.M., C.T., S.J.M., A.A., A.L., and S.A. performed research; V.B., G.J.B., M.P.J., H.R., G.J.L., and J.V. designed research; M.P.J., S.J.M., and G.C. contributed new reagents/analytic tools; and V.B., G.J.B., M.P.J., G.C., J.H., H.R., G.J.L., and J.V. wrote the paper.

Reviewers: J.B., University of Florida; B.D.B., National Institute for Communicable Diseases; and P.M., University of Basel.

The authors declare no conflict of interest.

Freely available online through the PNAS open access option.

See Commentary on page 9145.

[1]To whom correspondence may be addressed. Email: janet.hemingway@lstmed.ac.uk or vontas@imbb.forth.gr.

This article contains supporting information online at www.pnas.org/lookup/suppl/doi:10.1073/pnas.1608295113/-/DCSupplemental.

**Table 1. PRs of $C^{14}$-deltamethrin and comparable tarsal vs. topical application bioassays with deltamethrin on resistant (Res) and susceptible (Sus) *An. gambiae***

| | Insecticide assay | | | | | | |
|---|---|---|---|---|---|---|---|
| | | | Bioassay (95% confidence interval) | | | | |
| | | | | | Resistance ratio Res/Sus | | |
| Strain | PR, $10^{-3}$ (SD) | Ratio $PR_{Suc}/PR_{Res}$ | Tarsal $LC_{50} \times 10^{-4}$ | Topical $LC_{50} \times 10^{-4}$ | Tarsal | Topical | Ratio tarsal/topical |
| Sus | 60 (±14) | 2.06 | 0.29 (0.22–0.38) | 0.4 (0.1–1.1) | 22.41 (20.9–23.4) | 12.25 (7.3–28.0) | 1.83 |
| Res | 29 (±8)** | | 6.5** (4.6–8.9) | 4.9** (2.8–8.0) | | | |

$LC_{50}$, concentration resulting in the death of 50% of the test animals. $n = 3$ biological replicates; $^{**}P \leq 0.05$, Student's $t$ test.

role in insecticide resistance has been attributed to CYP4G17 and CYP4G16.

These P450 cytochromes are the only known members of the insect-specific 4G family of P450 cytochromes in *An. gambiae*. They are potential homologs of *Drosophila* dmCYP4G15 and dmCYP4G1. The latter has decarbonylase activity involved in the final step of cuticular hydrocarbon (CHC) biosynthesis from aldehyde precursors (21). In *Drosophila* dmCYP4G1 is localized in the CHC-secreting oenocytes in the abdomen, and dmCYP4G15 transcripts are enriched in the head and nervous system (21, 22). Both *An. gambiae cyp4g17* and *cyp4g16* transcripts are highly enriched in the abdominal integument (18).

Here we analyzed barriers to insecticide uptake through the cuticle by comparing the rate of internalization of radiolabeled pyrethroid and the response to different modes of insecticide application in resistant and sensitive strains of mosquitoes. We subsequently investigated possible cuticular modifications between resistant and susceptible mosquitoes by transmission electron microscopy (TEM) and quantitative GC/MS approaches. Finally, we analyzed the expression profile, subcellular localization, and activity of the *Anopheles* 4G P450 cytochromes to investigate their function in the CHC pathway and possible role in resistance.

## Results

**Insecticide Uptake Is Slower in Resistant Insects, and Resistance Is Partially By-Passed by Acetone/Topical Application.** Barriers to uptake were monitored initially by comparing the rate of internalization of a WHO standard oil-based formulation of radiolabeled insecticide after (tarsal) exposure on filter papers in the resistant and sensitive strains. By comparing radiolabeled $^{14}C$ extracted from the cuticle with residual $^{14}C$ in the whole mosquito, we observed that the internalization of deltamethrin was ~50% slower in resistant than in susceptible mosquitoes (Table 1). In addition, there was a 50% drop in the resistance ratio (from 22.4-fold to 12-fold) when the insecticide was applied topically in acetone as compared with the contact-exposure assay (Table 1).

**TEM Analysis of Cuticle Thickness.** To overcome issues in comparisons within and between samples, the apical region of the femur leg segment was analyzed. The same number of sections was taken in both samples, and measurements in each section (>10) were done randomly (Fig. 1*A*). The overall cuticle thickness was variable across legs but was significantly higher in the resistant strain (2.13 ± 0.32 μm) than in the sensitive strain (1.873 ± 0.30 μm) ($P < 0.05$) (Fig. 1*B*, *Left*). The thickness of epicuticle was much less variable and was significantly higher in the femur from resistant mosquitoes (resistant epicuticle = 0.57 μm ± 0.11 μm vs. susceptible epicuticle = 0.27 ± 0.04 μm; $P < 0.01$) (Fig. 1*B*, *Right*) and thus was the major contributor in the overall difference in the total thickness of the cuticle.

**Resistant *An. gambiae* Mosquitoes Contain Larger Amounts of CHC than Susceptible Specimens.** TLC analysis indicated that HCs were the most abundant components in the lipid layer of mosquito cuticle (Fig. 2*A*, *Inset*). GC analysis of CHCs and total mosquito HCs showed indistinguishable HC profiles by both GC-flame ionization detector (FID) and GC-MS (Fig. 2*A*), with CHCs representing 85.38 ± 0.99% of total HCs in resistant females and 81.91 ± 2.84% in susceptible females. A representative HC profile of adult *An. gambiae* is shown in Fig. 2*A* (also see Dataset S1). A previous report described 48 CHCs in *Anopheles coluzzii*, including n-alkanes, monomethyl, single-component dimethylalkanes, and small amounts of alkenes (23). Here, we extend this identification to 70 multicomponent peaks and identify a variety of multi-isomeric methyl- and dimethyl-branched components (Dataset S1). Saturated very-long-chain dimethyl- and monomethyl-branched components were the predominant structures. The relative abundance of multiple isomers of dimethyl-branched high-molecular-weight components, mostly of 39–47 odd-numbered carbon backbone, is remarkable (accounting for >50% of the HC blend). A multiplicity of 13,x-, 11,x-, and 15,x- isomers was found in most peaks, with x ranging mostly from 17 to 33 (Fig. 2*A* and Dataset S1), followed by a series of internally branched monomethylalkanes up to a C47 backbone, minor amounts of even-numbered dimethyl- and monomethyl-branched chains,

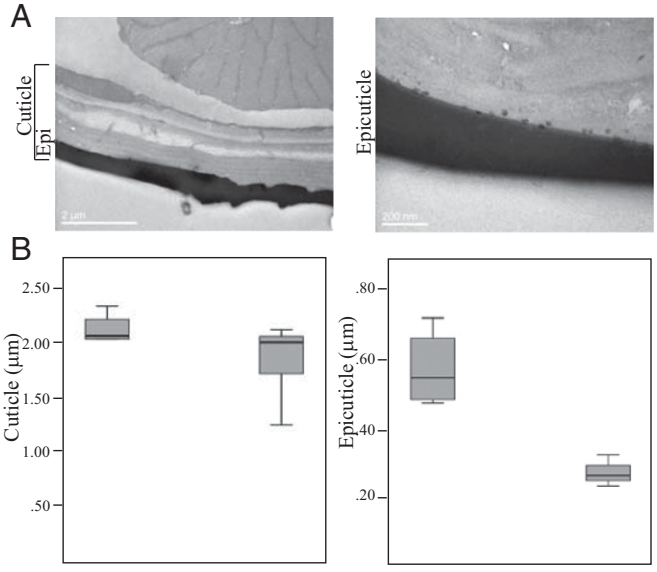


**Fig. 1.** TEM analysis of cuticle thickness. (*A*, *Left*) A representative image from a cross-section of the apical region of femur leg segment cuticle. The epicuticle (Epi) is the outermost gray zone. (*Right*) A higher-magnification image depicts numerous lipids or lipoprotein droplets deposited at the base of epicuticle (44). (*B*) Box-and-whisker plots of cuticle (*Left*) and epicuticle (*Right*) thickness. The boxes represent the 25% and 75% percentiles of five independent measurements for resistant (left box in each panel) and susceptible (right box in each panel) mosquitoes. The horizontal black line within the box indicates the mean.

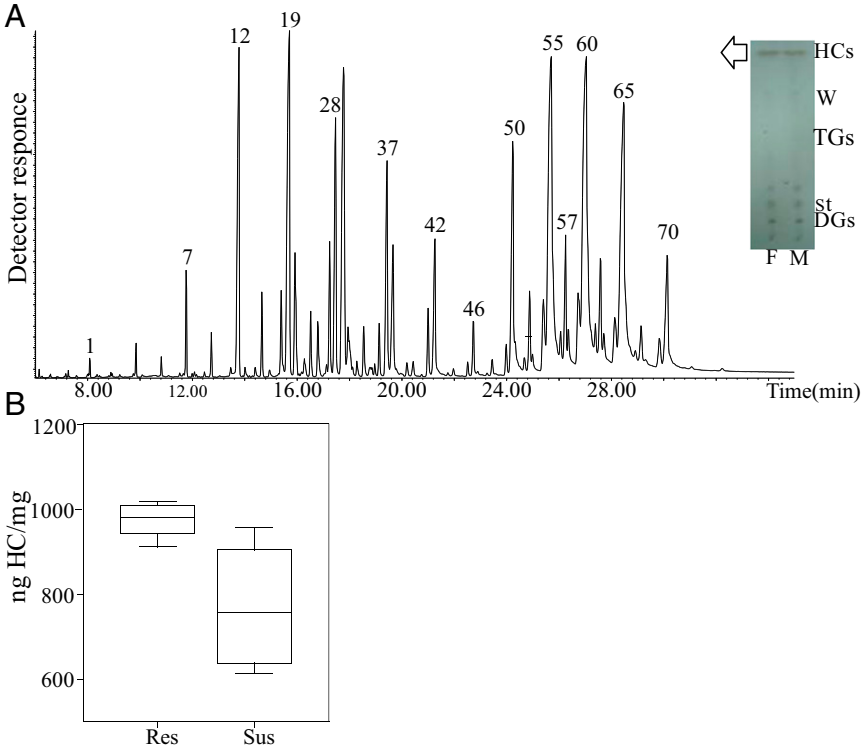


**Fig. 2.** Analysis of adult *An. gambiae* CHCs. (*A*) Representative total ion current (TIC) profile of *An. gambiae* HCs. Numbers indicating major HC peaks correspond to peak numbers from Dataset S1. (*Inset*) TLC for the separation of lipid species. Cuticular lipids from male (M) and female (F) mosquitoes were extracted by hexane and subsequently separated on 2D TLC. HCs are the major lipid species, compared with waxes (W), sterols (St), diglycerides (DGs), or triglycerides (TGs). First dimension of TLC: hexane; second dimension: hexane/diethyl ether/acetic acid. Visualization of lipids was performed after spraying the plates with 5% sulfuric acid in 95% ethanol, and charring at 180–200 °C for 20 min. (*B*) Comparison of CHCs in resistant (Res) and susceptible (Sus) females. The CHCs derived from resistant and susceptible adult (12- to 14-d-old) female mosquitoes were quantified by GC-MS/FID (20 insects pet vial) and were found to be significantly higher in resistant than in susceptible mosquitoes (980.5 ± 18.6 ng CHCs/mg of mosquito and 757.5 ± 72.5 ng CHCs/mg of mosquito, respectively). The box plots show the 25th and 75th percentile; the mean is shown as a black line within the box; error bars correspond to the 10th and 90th percentiles.

and odd-numbered straight-chain components from nC23 to nC33. Small amounts of straight-chain monounsaturated components up to 47 carbons, with double bonds located mostly in positions 9-, 7-, and other internal locations, were also identified.

Subsequently, CHCs derived from the resistant and the susceptible strains were compared. GC-FID analyses showed that, although there were no qualitative differences in the CHC profiles of resistant and susceptible female mosquitoes, the resistant mosquitoes contain significantly higher amounts (~29%) of CHCs than susceptible specimens (Fig. 2*B*).

**Association of the 4G Family of P450 Cytochomes with the CHC Production Pathway.** The finding of higher levels of CHCs in resistant mosquitoes supported a previous hypothesis that the increased expression of *Anopheles* 4G P450 cytochromes in resistant mosquitoes might be associated with up-regulation of the HC production pathway. To examine the function of the two *Anopheles* 4G P450 cytochromes found in the *Anopheles* genome, we undertook a series of experiments to identify cyp4g transcripts (Fig. S1), together with characterization of the subcellular localization and decarbonylase activity of the proteins encoded.

**CYP4G17 Is Dispersed Throughout Oenocyte Cytoplasm, Whereas CYP4G16 Is Associated with the Intracellular Side of the Plasma Membrane.** Longitudinal sections from frozen prefixed mosquito specimens were immunostained with α-CYP4G17–, α-CYP4G16–, and α-CPR–specific antibodies (green in Fig. 3*A*, *Left*). Both CYP4G16 and CYP4G17 gave very strong signals and thus were likely to be highly abundant in oenocytes (Fig. 3*A*), a cell type thought to secrete HCs. This group of cells, with a characteristic lobe shape, has previously been shown to express high levels of cytochrome P450 reductase (CPR), the obligatory P450 electron donor (24). We were unable to detect specific signals in other tissues by immunostaining.

Surprisingly, high-magnification confocal microscopy focusing on oenocytes revealed different subcellular distributions for CYP4G17 and CYP4G16 (Fig. 3*B*); CYP4G17 resides throughout the intracellular region, similar to CPR, as expected from a microsomal P450 protein, whereas CYP4G16 is found at the periphery of the oenocyte cell, presumably associated with the plasma membrane (PM). The specificity of the antibody was checked by silencing the corresponding gene, followed by immunofluorescence (Fig. S2*A*), and further immunofluorescence experiments in the presence or absence of detergent (± Triton X-100) (25) demonstrated that CYP4G16 is associated with the PM intracellularly (Fig. S2*B*).

**CYP4G16 Encodes a Functional Oxidative Decarbonylase.** To provide direct evidence of HC synthesis involvement through an in vitro decarbonylase assay, CYP4G16 and CYP4G17 were expressed as fusion proteins with CPR (from housefly) in Sf9 (insect) cells using a baculovirus expression system similar to that described by Qiu et al. (21). As shown in Fig. 4*A*, the CYP4G16 fusion preparation converted C18 aldehyde to HC with efficiency similar to that of the housefly CYP4G2 protein and showed time-dependent decarbonylase activity with this substrate (Fig. 4*B*). A similar fusion protein, CYP4G17, was produced at a lower concentration than CYP4G16 and did not demonstrate aldehyde decarbonylase activity with the C18 aldehyde substrate (Fig. 4*A*). Longer aldehydes could not be tested because of solubility and the unavailability of labeled substrate.

## Discussion

The reduced penetration rate of $^{14}$C deltamethrin in a highly resistant strain of *An. gambiae* suggests that cuticular modification may affect insecticide uptake. Similarly, reduced deltamethrin penetration was observed in a *T. infestans* resistant strain (10), in which removal of the epicuticle lipid layer with solvents correlated with enhanced insecticide penetration and insect mortality (26). A slower rate of penetration into the mosquito may enhance resistance by increasing the time available for metabolic processes to inactivate the insecticide before it reaches the target site. Possible cuticular modifications might include changes in the thickness of the cuticle or qualitative modification of its components. In the strains examined, resistant mosquitoes had a thicker epicuticle layer than susceptible mosquitoes and contained greater quantities of CHCs, but qualitative CHC profiles were not altered. The

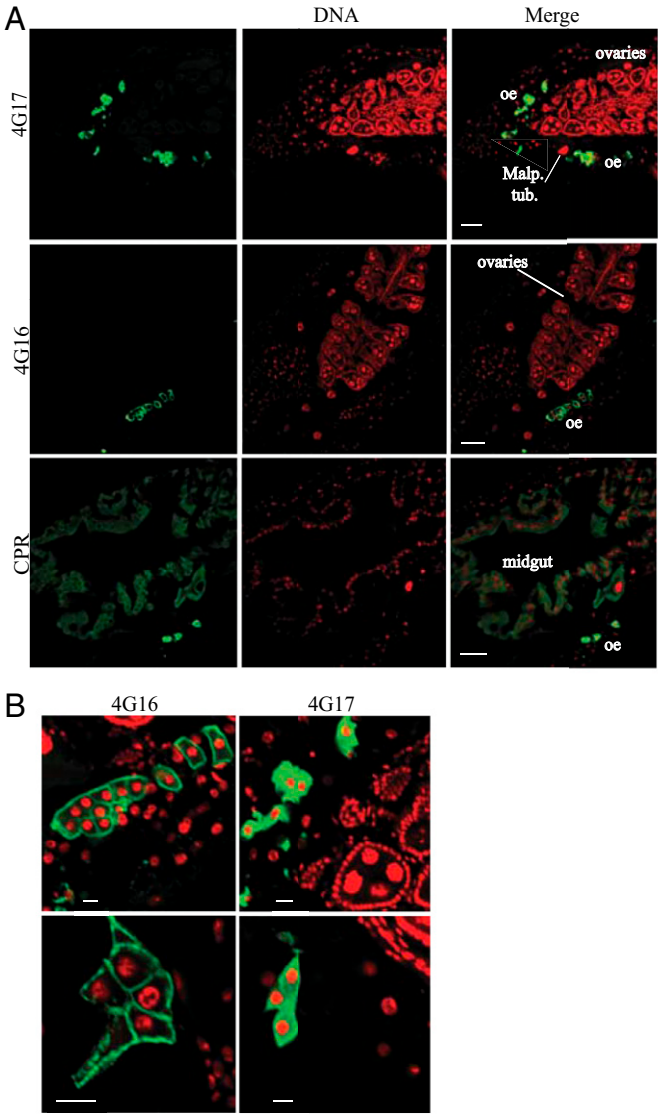


**Fig. 3.** Immunohistochemical localization of *An. gambiae* 4G P450 cytochromes. (*A*, *Left* column) Longitudinal sections from mosquito specimens were immunostained with α-CYP4G17–, α-CYP4G16–, or α-CPR–specific antibodies (green), respectively. (*Center* column) Cell nuclei are stained red with TOPRO. (*Right* column) Merged immunohistochemical images of P450 and nuclei staining. (Scale bars, 50 μm.) Malp. tub., Malpighian tubules; oe, oenocytes. (*B*) Merged immunohistochemical images as in *A* focusing on oenocytes, showing the subcellular localization of CYP4G17 in the cytoplasm (presumably bound to ER) and CYP4G16 associated with PM. (Scale bars, 10 μm.)

possibility that differences in the size of individuals or in their genetic background might introduce variability in cuticle thickness measurements cannot be excluded, although the average weight of the resistant and the susceptible mosquitoes was not different (resistant = 1.07 ± 0.118 mg; susceptible = 1.14 ± 0.102 mg, $n$ = ~500), and both strains were of the same molecular form and originated from West Africa.

Interestingly, adult *An. gambiae* have a considerably higher CHC/weight ratio (~300–400 ng/mg) than reported for *T. infestans* (30–40 ng/mg) (11). In addition, in *An. gambiae* CHCs represent the majority (>80%) of the total mosquito HCs, with a composition similar to that of the internal pool. In insects such as triatomines and cockroaches, only ~10–20% of the HCs are transported to the surface, and the majority of the methyl-branched HCs are retained in the hemolymph as reservoir (27, 28).

In addition, the *An. gambiae* strains examined have a distinct and remarkable abundance of very-long-chain methyl-branched HCs (VLCMHCs) compared with other insects examined to date (29). VLCMHCs have been associated with increased waterproofing properties (30) and may be correlated with a need for greater desiccation resistance in these relatively small insects.

Quantitative GC/MS on whole-body extracts from pools of mosquitoes showed that resistant mosquitoes contain more CHCs than susceptible strains, as had been shown in similar studies with *T. infestans* (10, 11). We hypothesized that increased HC production in resistant *Anopheles* might be associated with increased expression of CYP4G16 and/or CYP4G17 and might contribute to resistance by changing the permeability and insecticide-uptake rate (16). To investigate the potential function of the two 4G P450 cytochromes, we defined their localization and in vitro oxidative decarbonylase activity.

Previous transcriptomic analysis of dissected mosquitoes indicated high levels of cyp4g16 and cyp4g17 mRNA in the abdominal integument (18). We now show that within this abdominal region the respective proteins are highly abundant in oenocyte cells, which are known to produce and secrete HCs in other insects (21, 31, 32). The two P450 cytochromes have different subcellular localizations: CYP4G17 was found throughout the intracellular compartment, as expected for a general endoplasmic reticulum (ER)-bound P450 protein (similar to CPR), and CYP4G16 was predominantly associated with the cytoplasmic side of the cell membrane. We cannot be sure whether this localization is within the PM or is part of the distal ER that may associate closely with the PM (33). This site appears to be unique for a P450. A small number of mammalian P450 cytochromes have been localized within PMs. However, in these cases the major location site remains on the ER (34). Furthermore, these mammalian membrane-bound P450 cytochromes have catalytic surfaces facing the extracellular space (35, 36).

The different localization of the two P450 cytochromes may indicate differences in CYP4G16 and CYP4G17 cellular functions. One possible scenario could be that the proteins display different substrate specificities. So far, only CYP4G16 has been found to have in vitro decarbonylase activity against a C18 aldehyde substrate to produce HCs. Our efforts characterize the function of CYP4G17 fully were inconclusive, mainly because the protein was not stably expressed. However, we cannot rule out the possibility that CYP4G17 (and CYP4G16) can catalyze the conversion of lipids of different molecular weights and/or carrying methyl-branched precursors.

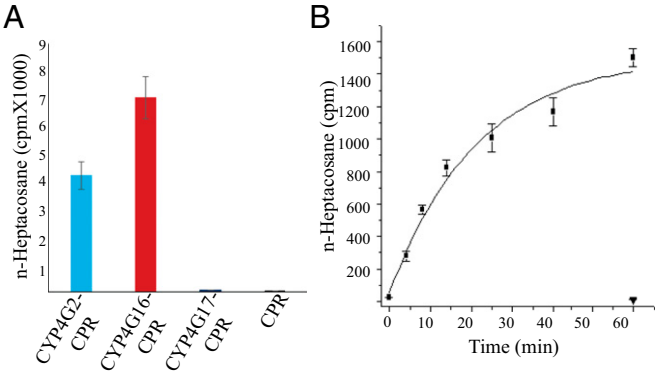


**Fig. 4.** Decarbonylase activity of microsomal CYP4G16-CPR fused protein. (*A*) Conversion of [9,10]$^3$H-octadecanal to n-heptacosane after 1-h incubation. CYP4G2-CPR is the positive control (21). Values are shown as means ± SE; $n$ = 3. (*B*) In vitro expression and decarbonylase activity of microsomal CYP4G16-CPR fused protein: effect of time on the conversion of tritiated octadecanal to n-heptadecane. Filled squares, CYP4G16-CPR; inverted triangle, CPR control. Values are shown as means ± SE; $n$ = 3. cpm, Counts per minute.

Given its putative role in epicuticular lipid biosynthesis, the finding that *Anopheles* CYP4G16 protein exerts its decarbonylase activity associated with the PM is intriguing. The biosynthetic machinery responsible for lipid metabolism and the production of CHCs in other insects is thought to be localized on the smooth ER (37, 38), although there are exceptions (39). Further studies are needed to establish the localization of the other CHC enzyme machinery in *An. gambiae*, including elongases, desaturases, and reductases that would be expected to reside in the oenocytes. Our working hypothesis is that newly synthesized, very hydrophobic CHCs could be manufactured and loaded directly onto lipophorin at the lipophilic interface of the cell membrane for transport to the cuticle (32, 40). In addition to the biosynthetic enzymes, an electron donor, such as the ER-bound CPR, is necessary for P450 activity. These studies indicate a degree of positional overlap of CPR with CYP4G16, indicating that CPR may well retain its function as an electron donor with P450 cytochromes in this PM-associated location (Fig. S2*C*).

A functional in vivo link between the CYP4G16 and the synthesis of epicuticular lipids was not observed following *cyp4g16* RNAi silencing. Although diminishing the oenocyte-expressed protein was successful at the adult stage (Fig. S2*A*), no significant differences were observed in CHC content or composition. One possibility is that CHC biosynthesis is less active in adult oenocytes, and large deposits of CHC are generated during the late larval and pupal stages. The application of RNAi at earlier (pupal or larval) stages was not feasible, and it is likely that a transgenic approach to manipulate CYP4G16 and CYP4G17, specifically at earlier mosquito stages, is needed to elucidate this issue.

Together the data suggest a role of CYP4G16 in insecticide resistance via enrichment of the CHC content, thus reducing pyrethroid uptake. The cuticular-based resistance mechanism, in addition to targeting site resistance and detoxification, further strengthens the insecticide resistance phenotype and potentially broadens it to multiple insecticide classes, thus providing additional challenges to resistance management. The Tiassale strain used in this study is one of the most highly resistant field strains of *An. gambiae*, with resistance encompassing all currently used classes of public health insecticides (4). Selection for and spread of such broad-spectrum mechanisms should be avoided; otherwise, resistance to insecticides could have a massive impact on our ability to prevent malaria and other vector-borne diseases.

## Materials and Methods

**Mosquito Strains and Bioassays.** The *An. gambiae* strain N'Gusso, from Cameroon, is susceptible to all classes of insecticide. The Tiassale strain, from southern Cote d'Ivoire, is resistant to all insecticide classes (4). Mosquitoes were reared under standard insectary conditions at 27 °C and 70–80% humidity under a 12-h:12-h photoperiod. Bioassays, including tarsal contact and topical application of the insecticide deltamethrin, were conducted as previously described (41), with minor modifications. For tarsal contact exposure, 10–13 mosquitoes were exposed to the coated surface of a Petri dish. For topical application, mosquitoes were briefly anesthetized using $CO_2$, and 0.25 μL of insecticide solubilized in acetone was carefully applied to the dorsal thorax using a Burkard hand microapplicator (Burkard Scientific). Five replicates of 10 mosquitoes were exposed to each insecticide concentration. After exposure, mosquitoes were maintained at 27 ± 2 °C and 70 ± 5% relative humidity with access to a 10% (wt/vol) sucrose solution. Mortality was assessed 24 h after exposure.

**Penetration Rate of $^{14}$C Deltamethrin.** Thirty to thirty-five female mosquitoes from each strain were exposed for 3 min to radiolabeled 0.01% deltamethrin, donated by Ralf Nauen, Bayer CropScience, Monheim am Rhein, Germany, on impregnated filter paper, using standard WHO bioassay protocols (apps.who.int/iris/bitstream/10665/64879/1/WHO_CDS_CPC_MAL_98.12.pdf). At the end of the exposure, mosquitoes were collected and rinsed three times with 1 mL hexane. The washes were retained. Mosquitoes were allowed to dry before homogenization in 500 μL PBS. Ten milliliters of liquid Scintillation Counting Mixture (Ultima Gold; 6013326; PerkinElmer) was added to each sample, and the corresponding counts per minute were measured on a beta counter (LS1701; Beckman). The penetration rate (PR) was calculated as the ratio of internal counts per minute to total counts per minute.

**TEM.** The apical regions of the femur leg segment of 25 susceptible and 25 resistant female mosquitoes were dissected and fixed in 2% (vol/vol) glutaraldehyde, 2% (vol/vol) paraformaldehyde in 0.1 M sodium cacodylate buffer (SCB), pH 7.4, for 24 h at 4 °C with constant rotation. The samples were washed three times for 5 min each in 0.1 M SCB, postfixed in 1% aqueous $OsO_4$ for 12 h at room temperature with constant rotation, and then washed again as above. After the last washing, the samples were stained with 2% (vol/vol) uranil acetate for 1 h. Then the samples were rinsed with SCB, dehydrated through an ascending acetone gradient [30–50–70–90–100% (vol/vol)], infiltrated with Durcupan ACM Fluka resin [3:1 propylene oxide: resin mixture for 1 h followed by a 1:1 and a 1:3 propylene oxide:resin mixture for 1 h each and finally 100% (vol/vol) resin for 16 h], and embedded in flat molds. The resin was cured in a drying oven at 60 °C for 48 h. Samples were trimmed, thin-sectioned (gold section), and absorbed onto 300-mesh copper grids. Observation was carried out using a high-resolution JEM 2-100 transmission electron microscope (JEOL) at an operating voltage of 80 kV.

**Extraction of Lipids, Separation by TLC, HC Fractionation, and Derivatization.** Cuticular lipids from female mosquito specimens were extracted by three 1-min immersions in hexane with gentle agitation, and extracts were pooled and evaporated under a $N_2$ stream (20 insects per tube, $n = 5$ resistant and $n = 4$ susceptible). Internal HCs were further extracted from the same samples after 24-h immersion in 2.5 mL hexane and a final hexane washing (2 mL). Total HCs were extracted in the same way without prior extraction of cuticular lipids. The lipid extracts were analyzed by TLC on 4 × 8 cm Polygram Sil G/UV254 silica gel plates (Macherey-Nagel) using two development solvent mixtures: n-hexane [100% (vol/vol)], followed by n-hexane:ethyl ether:acetic acid [80:20:1 (vol/vol)]. Plates were sprayed with 5% sulfuric acid in 95% (vol/vol) ethanol, and lipid bands were visualized after charring at 180–200 °C for 20 min. HCs were separated from other components by adsorption chromatography on a minicolumn (2.5 × 0.5 cm i.d.) of activated SUPELCOSIL A (Supelco), eluted with hexane (4 mL), and then concentrated under an $N_2$ atmosphere. Double-bond location was detected after derivatization of the HCs according to Carlson et al. (42). Total HC extracts obtained from 100 susceptible female mosquitoes were solved in hexane (100 μL) and treated with 100 μL of dimethyl disulfide and 50 μL of iodine solution in diethyl ether (60 mg/mL). The reaction mixture was held for 4 h at 40 °C, diluted with 0.5 mL of hexane, and treated with $Na_2S_2O_3$ 10% (wt/vol) (Merck) until the iodine color disappeared. The organic phase then was separated and evaporated under $N_2$.

**CHC Quantitation and Identification by GC and GC/MS.** GC analyses were performed using a Hewlett-Packard 6890 gas chromatograph with an FID and equipped with a split/splitless injector port, fitted with a high-temperature capillary column (30 m L × 0.25 mm i.d., 0.25 μm film thickness) (Zebron ZB-5HT Inferno; Phenomenex). The oven temperature was programmed to increase from 50 °C (hold time 2 min) to 180 °C in increments of 20 °C/min and then from 180 °C to 330 °C in increments of 3 °C/min (hold time 10 min). The relative amount (mean value ± SD) of each component was calculated by dividing the corresponding peak area by the total HC peak area. Quantitative amounts were estimated by coinjection of nC24 as an internal standard (28 ng per sample). GC-MS analyses were performed using the GC equipment and column described for GC-FID analysis, coupled to a mass-selective detector (MSD) (Agilent model 5975C VL). The injector port was operated in splitless mode at 360 °C, and the oven temperature was programmed to increase from 50 °C (hold time 1 min) to 200 °C in increments of 50 °C/min and then to 360 °C in increments of 7 °C/min, with a holding time of 20 min. The carrier gas was helium, at 11.36 psi, with a linear velocity of 39 cm/s. The MSD was operated in the SCAN mode with a mass range of 35–850 atomic mass units, electron impact mode at 70 eV, and transfer line at 360 °C; the ionization chamber was operated at 280 °C (43). Methyl branching assignment was based on their mass fragmentation pattern and Kovats index values, estimated after injection of n-alkane standards, of 22–44 carbons (Sigma Aldrich) (43). Shorthand nomenclature to identify the HCs used in the text and tables is as follows: CXX indicates the total number of carbons in the straight chain; linear alkanes are denoted as n-CXX; the location of methyl branches is described as x-Me for monomethyl alkanes and as x,x-DiMe for dimethyl alkanes. Alkenes are shown as x-CXX:1.

**Raising of Antibodies.** Rabbit polyclonal antibodies targeting a recombinant CYP4G16 peptide were made and affinity purified by Davids Biotechnologie. The sequence encoding the peptide (LRHRKMWLYPDLFFNLTQYAKKQVKLLNTIHSLTKKVIRNKKAAFDTGTRGSLATTSINTVNIEKSKSDSTKTNTVEGLSFG) was cloned using the primers Fab16 and Rab16 (Table S1), expressed in bacteria with a 6xHis tag at the N terminus, and affinity purified to homogeneity by Ni-NTA$^{2+}$ chromatography. The purified peptide was used as an antigen to develop antibodies

in rabbits. The specific antibodies that were used for the detection of the CYP4G17 (AGAP000877) and the CPR proteins (AGAP000500) have been previously described in refs. 18 and 24, respectively.

**Immunofluorescence and Confocal Microscopy.** Three- to five-day-old sugar-fed female mosquitoes were fixed in a cold solution of 4% formaldehyde (methanol free; Thermo Scientific) in PBS for 4 h, cryoprotected in 30% (wt/vol) sucrose/PBS at 4 °C for 12 h, immobilized in Optimal Cutting Temperature (OCT) compound (Tissue-Tek; Sakura), and stored at −80 °C until use. Immunofluorescence analysis, followed by confocal microscopy, was performed on longitudinal sections of the frozen prefixed mosquito specimens as described in ref. 18.

**Functional Expression of 4G P450 Cytochromes.** The 4G16-CPR and 4G17-CPR fusion protein consists of the full-length corresponding P450 cytochromes fused via a Ser–Ser dipeptide to the catalytic domain of housefly CPR (amino acids 51–671; GenBank accession no. AAA29295.1). The clone was constructed by Gibson assembly using the In-Fusion kit (Clontech). The pENTR_4G2-CPR plasmid was divergently amplified as previously described (21). The ORFs of CYP4G16PA (vector base: AGAP001076-PA) and CYP4G17 (vector base: AGAP000877-PA) codon-optimized for Sf9 cells and with flanking pENTR4R5ic and CPRfusF2ic linkers were synthesized by Biomatik. The CYP4G16PA_Sf9 and CYP4G17_Sf9 bias fragments were amplified using pENTR4R5ic and CPRfusF2ic primers (Table S1) with CloneAmp HiFi PCR Premix as above. The profile was 34 cycles at 98 °C for 10 s, 55 °C for 15 s, and 72 °C for 10 s. The pENTR_4G16PA_Sf9, pENTR_4G17_Sf9 bias fragments and the pENTR4_CPR fragment were verified by gel electrophoresis, copurified with a NucleoSpin Gel and PCR Clean-up (Machery-Nagel), assembled by In-Fusion cloning in 10-μL reactions, transformed into Stellar-competent *Escherichia coli* (Clontech), and selected on LB kanamycin plates. Recombinant clones were identified by PCR and sequenced to confirm the integrity of the insert. Recombinant proteins were produced in Sf9 cells using the Baculo-Direct expression system (Invitrogen), as previously described (21). CYP4G16PA-CPR and CYP4G17-CPR were quantitated by CO-difference spectrum analysis using a microplate format (21). Octadecanal (substrate) was prepared, and oxidative decarbonylase assays were performed as described in ref. 21.

**Statistical Analysis.** Statistics were obtained with GraphPad Prism software, version 5.03. Differences in the total HC amounts and the thickness were analyzed with Student's *t* test.

**ACKNOWLEDGMENTS.** We thank Dr. Evangelia Morou (University of Crete) and Fotini Tanka for help with initial experiments on the uptake of radiolabeled deltamethrin and the stainings, respectively; Sevasti Papadogiorgaki for help with TEM; and Prof. Feyereisen (University of Ghent) for helpful suggestions during this project. This work was funded by the European Union Seventh Framework Programme FP7 (2007–2013) under Grant Agreement 265660 AvecNet.

1. Toé KH, et al. (2014) Increased pyrethroid resistance in malaria vectors and decreased bed net effectiveness, Burkina Faso. *Emerg Infect Dis* 20(10):1691–1696.
2. Ranson H, Lissenden N (2016) Insecticide resistance in African *Anopheles* MOSQUITOES: A worsening situation that needs urgent action to maintain malaria control. *Trends Parasitol* 32(3):187–196.
3. Liu N (2015) Insecticide resistance in mosquitoes: Impact, mechanisms, and research directions. *Annu Rev Entomol* 60(60):537–559.
4. Edi CVA, Koudou BG, Jones CM, Weetman D, Ranson H (2012) Multiple-insecticide resistance in *Anopheles gambiae* mosquitoes, Southern Côte d'Ivoire. *Emerg Infect Dis* 18(9):1508–1511.
5. Ranson H, et al. (2009) Insecticide resistance in *Anopheles gambiae*: Data from the first year of a multi-country study highlight the extent of the problem. *Malar J* 8:299.
6. Hemingway J, et al. (2016) Averting a malaria disaster: Will insecticide resistance derail malaria control? *Lancet* 387(10029):1785–1788.
7. Ahmad M, Denholm I, Bromilow RH (2006) Delayed cuticular penetration and enhanced metabolism of deltamethrin in pyrethroid-resistant strains of *Helicoverpa armigera* from China and Pakistan. *Pest Manag Sci* 62(9):805–810.
8. Gunning RV, Ferris IG, Easton CS (1994) Toxicity, penetration, tissue distribution, and metabolism of methyl parathion in *Helicoverpa armigera* and *H. punctigera* (Lepidoptera: Noctuidae). *J Econ Entomol* 87(5):1180–1184.
9. Lin YY, Jin T, Jin QA, Wen HB, Peng ZQ (2012) Differential susceptibilities of *Brontispa longissima* (Coleoptera: Hispidae) to insecticides in Southeast Asia. *J Econ Entomol* 105(3):988–993.
10. Juárez MP, Pedrini N, Girotti JR, Mijailovsky SJ (2010) Pyrethroid resistance in Chagas disease vectors: The case of *Triatoma infestans* cuticle. *Resistance Pest Management* 01(19):59–61.
11. Pedrini N, et al. (2009) Control of pyrethroid-resistant Chagas disease vectors with entomopathogenic fungi. *PLoS Negl Trop Dis* 3(5):e434.
12. Strycharz JP, et al. (2013) Resistance in the highly DDT-resistant 91-R strain of *Drosophila melanogaster* involves decreased penetration, increased metabolism, and direct excretion. *Pestic Biochem Physiol* 107(2):207–217.
13. Wood O, Hanrahan S, Coetzee M, Koekemoer L, Brooke B (2010) Cuticle thickening associated with pyrethroid resistance in the major malaria vector *Anopheles funestus*. *Parasit Vectors* 3:67.
14. Vontas J, et al. (2007) Transcriptional analysis of insecticide resistance in *Anopheles stephensi* using cross-species microarray hybridization. *Insect Mol Biol* 16(3):315–324.
15. Gregory R, et al. (2011) A de novo expression profiling of *Anopheles funestus*, malaria vector in Africa, using 454 pyrosequencing. *PLoS One* 6(2):e17418.
16. Jones CM, et al. (2013) The dynamics of pyrethroid resistance in *Anopheles arabiensis* from Zanzibar and an assessment of the underlying genetic basis. *Parasit Vectors* 6:343.
17. Toé KH, N'Falé S, Dabiré RK, Ranson H, Jones CM (2015) The recent escalation in strength of pyrethroid resistance in *Anopheles coluzzi* in West Africa is linked to increased expression of multiple gene families. *BMC Genomics* 16:146.
18. Ingham VA, et al. (2014) Dissecting the organ specificity of insecticide resistance candidate genes in *Anopheles gambiae*: Known and novel candidate genes. *BMC Genomics* 15(1):1018.
19. Müller P, et al. (2008) Field-caught permethrin-resistant *Anopheles gambiae* overexpress CYP6P3, a P450 that metabolises pyrethroids. *PLoS Genet* 4(11):e1000286.
20. David JP, Ismail HM, Chandor-Proust A, Paine MJ (2013) Role of cytochrome P450s in insecticide resistance: Impact on the control of mosquito-borne diseases and use of insecticides on Earth. *Philos Trans R Soc Lond B Biol Sci* 368(1612):20120429.
21. Qiu Y, et al. (2012) An insect-specific P450 oxidative decarbonylase for cuticular hydrocarbon biosynthesis. *Proc Natl Acad Sci USA* 109(37):14858–14863.
22. Maïbèche-Coisne M, Monti-Dedieu L, Aragon S, Dauphin-Villemant C (2000) A new cytochrome P450 from *Drosophila melanogaster*, CYP4G15, expressed in the nervous system. *Biochem Biophys Res Commun* 273(3):1132–1137.
23. Caputo B, et al. (2005) Identification and composition of cuticular hydrocarbons of the major Afrotropical malaria vector *Anopheles gambiae* s.s. (Diptera: Culicidae): Analysis of sexual dimorphism and age-related changes. *J Mass Spectrom* 40(12):1595–1604.
24. Lycett GJ, et al. (2006) *Anopheles gambiae* P450 reductase is highly expressed in oenocytes and in vivo knockdown increases permethrin susceptibility. *Insect Mol Biol* 15(3):321–327.
25. Loeper J, Le Berre A, Pompon D (1998) Topology inversion of CYP2D6 in the endoplasmic reticulum is not required for plasma membrane transport. *Mol Pharmacol* 53(3):408–414.
26. Juárez MP (1994) Inhibition of cuticular lipid synthesis and its effect on insect survival. *Arch Insect Biochem Physiol* 25(3):177–191.
27. Young HP, Bachmann JAS, Sevala V, Schal C (1999) Site of synthesis, tissue distribution, and lipophorin transport of hydrocarbons in *Blattella germanica* (L.) nymphs. *J Insect Physiol* 45(4):305–315.
28. Juárez MP, Fernández GC (2007) Cuticular hydrocarbons of triatomines. *Comp Biochem Physiol A Mol Integr Physiol* 147(3):711–730.
29. Dweck HK, et al. (2015) Pheromones mediating copulation and attraction in *Drosophila*. *Proc Natl Acad Sci USA* 112(21):E2829–E2835.
30. Gibbs A, Pomonis JG (1995) Physical-properties of insect cuticular hydrocarbons—The effects of chain-length, methyl-branching and unsaturation. *Comp Biochem Physiol B* 112(2):243–249.
31. Wigglesworth VB (1970) Structural lipids in the insect cuticle and the function of the oenocytes. *Tissue Cell* 2(1):155–179.
32. Makki R, Cinnamon E, Gould AP (2014) The development and functions of oenocytes. *Annu Rev Entomol* 59:405–425.
33. Helle SC, et al. (2013) Organization and function of membrane contact sites. *Biochim Biophys Acta* 1833(11):2526–2541.
34. Neve EPA, Ingelman-Sundberg M (2008) Intracellular transport and localization of microsomal cytochrome P450. *Anal Bioanal Chem* 392(6):1075–1084.
35. Wu D, Cederbaum AI (1992) Presence of functionally active cytochrome P-450IIE1 in the plasma membrane of rat hepatocytes. *Hepatology* 15(3):515–524.
36. Loeper J, et al. (1993) Cytochromes P-450 in human hepatocyte plasma membrane: Recognition by several autoantibodies. *Gastroenterology* 104(1):203–216.
37. Serra M, Piña B, Abad JL, Camps F, Fabriàs G (2007) A multifunctional desaturase involved in the biosynthesis of the processionary moth sex pheromone. *Proc Natl Acad Sci USA* 104(42):16444–16449.
38. Hagström AK, Walther A, Wendland J, Löfstedt C (2013) Subcellular localization of the fatty acyl reductase involved in pheromone biosynthesis in the tobacco budworm, *Heliothis virescens* (Noctuidae: Lepidoptera). *Insect Biochem Mol Biol* 43(6):510–521.
39. Chung H, Carroll SB (2015) Wax, sex and the origin of species: Dual roles of insect cuticular hydrocarbons in adaptation and mating. *BioEssays* 37(7):822–830.
40. Gutierrez E, Wiggins D, Fielding B, Gould AP (2007) Specialized hepatocyte-like cells regulate *Drosophila* lipid metabolism. *Nature* 445(7125):275–280.
41. Marcombe S, et al. (2009) Exploring the molecular basis of insecticide resistance in the dengue vector *Aedes aegypti*: A case study in Martinique Island (French West Indies). *BMC Genomics* 10:494.
42. Hollingsworth RI, Carlson RW (1989) 27-Hydroxyoctacosanoic acid is a major structural fatty acyl component of the lipopolysaccharide of Rhizobium trifolii ANU 843. *J Biol Chem* 264(16):9300–9303.
43. Girotti JR, Mijailovsky SJ, Juarez MP (2012) Epicuticular hydrocarbons of the sugarcane borer *Diatraea saccharalis* (Lepidoptera: Crambidae). *Physiol Entomol* 37(3):266–277.
44. Wigglesworth VB (1975) Incorporation of lipid into the epicuticle of *Rhodnius* (Hemiptera). *J Cell Sci* 19(3):459–485.